

Review

Advanced Algorithms for Low Dimensional Metal Oxides-Based Electronic Nose Application: A Review

Xi Wang^{1,2,†}, Yangming Zhou^{1,2,†}, Zhikai Zhao^{1,2,*}, Xiujian Feng³, Zhi Wang⁴ and Mingzhi Jiao^{1,2,4,*}

¹ National and Local Joint Engineering Laboratory of Internet Application Technology on Mine, China University of Mining and Technology, Xuzhou 221116, China; ts22060015a31@cumt.edu.cn (Y.Z.)

² School of Information and Control Engineering, China University of Mining and Technology, Xuzhou 221116, China

³ School of Mines, China University of Mining and Technology, Xuzhou 221116, China

⁴ School of Safety Engineering, China University of Mining and Technology, Xuzhou 221116, China

* Correspondence: zhikaizhao@163.com (Z.Z.); mingzhijiao@cumt.edu.cn (M.J.);
Tel.: +86-136-8514-6374 (Z.Z.); +86-139-5220-4541 (M.J.)

† These authors contributed equally to this work.

Abstract: Low-dimensional metal oxides-based electronic noses have been applied in various fields, such as food quality, environmental assessment, coal mine risk prediction, and disease diagnosis. However, the applications of these electronic noses are limited for conditions such as precise safety monitoring because electronic nose systems have problems such as poor recognition ability of mixed gas signals and sensor drift caused by environmental factors. Advanced algorithms, including classical gas recognition algorithms and neural network-based algorithms, can be good solutions for the key problems. Classical gas recognition methods, such as support vector machines, have been widely applied in electronic nose systems in the past. These methods can provide satisfactory results if the features are selected properly and the types of mixed gas are under five. In many situations, this can be challenging due to the drift of sensor signals. In recent years, neural networks have undergone revolutionary changes in the field of electronic noses, especially convolutional neural networks and recurrent neural networks. This paper reviews the principles and performances of typical gas recognition methods of the electronic nose up to now and compares and analyzes the classical gas recognition methods and the neural network-based gas recognition methods. This work can provide guidance for research in related fields.

Keywords: low-dimensional metal oxides; gas recognition algorithm; electronic noses; gas sensor array; machine learning; deep learning



Citation: Wang, X.; Zhou, Y.; Zhao, Z.; Feng, X.; Wang, Z.; Jiao, M. Advanced Algorithms for Low Dimensional Metal Oxides-Based Electronic Nose Application: A Review. *Crystals* **2023**, *13*, 615. <https://doi.org/10.3390/cryst13040615>

Academic Editors: Hu Li, Klaus Leifer and Paolo Olivero

Received: 21 February 2023

Revised: 24 March 2023

Accepted: 27 March 2023

Published: 3 April 2023



Copyright: © 2023 by the authors. Licensee MDPI, Basel, Switzerland. This article is an open access article distributed under the terms and conditions of the Creative Commons Attribution (CC BY) license (<https://creativecommons.org/licenses/by/4.0/>).

1. Introduction

Electronic nose systems have been developed for 40 years since Persaud et al. first put forward an electronic nose based on biological olfactory senses in 1982 [1]. An electronic nose system is a set of electronic equipment simulating animal or human olfactory systems for the qualitative and quantitative composition of gas, also known as an artificial olfactory system. The working procedure of the electronic nose shown in Figure 1 includes four processes: data acquisition, data processing, model comparison, and identification decision [2]. With the great progress of core technologies, for instance, semiconductors, integrated circuits, and artificial intelligence, electronic nose technology has also been rapidly developed. Based on low-dimensional metal oxides, very advanced electronic nose systems can be developed [3–8]. The response mechanism of a metal oxide gas sensor includes three parts: receiving, transducing, and utilization. The latest metal oxide sensitive layer is usually made of low-dimensional metal oxide material, which has higher sensitivity, selectivity, and response speed than a traditional metal oxide microstructure. Its working mechanism is similar to the traditional metal oxide gas sensor. When the target gas is in contact with

the sensitive layer, it causes a REDOX reaction, a change in concentration of the surface adsorbed oxygen ion, thereby changing the charge state on the surface of the sensitive layer, resulting in changes in the resistance value of the sensitive layer. Low-dimensional metal oxides have a higher specific surface area and more surface active sites, so they can better adsorb gas molecules and improve detection sensitivity. Low-dimensional metal oxide materials also typically have faster response and recovery due to their conductive properties being affected by surface effects, thus, immediately changing resistance values upon the adsorption of gas molecules to the surface, resulting in a faster response to the presence of the target gas. An electronic nose can realize the rapid and accurate detection of a gas mixture. They are widely applied in various fields, for instance, disease diagnosis [9–13], food quality [14–16], environmental monitoring [17,18], coal mine risk assessment [19], etc. A number of recent studies have shown that electronic noses can also be used in the detection of COVID-19 [20–22].

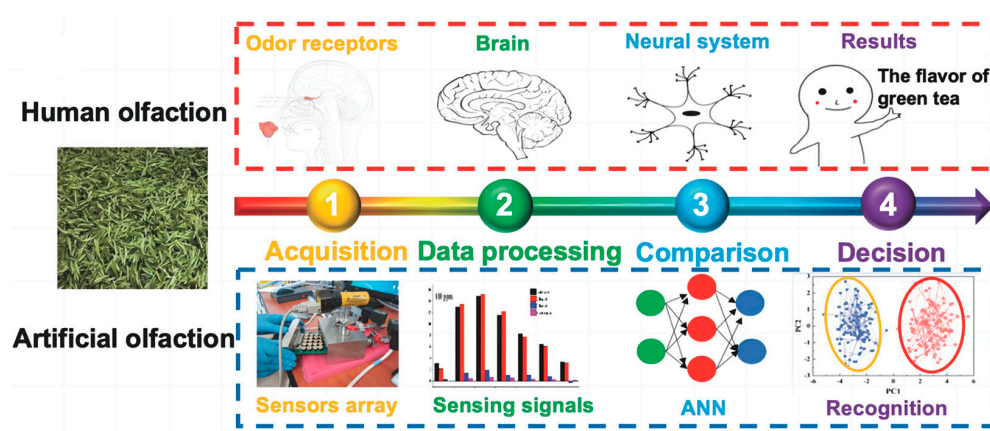


Figure 1. Schematic diagram of the human olfaction and e–nose system in 2022 [2].

Early gas recognition methods usually used artificial sensory recognition, gas chromatography [23], and laser spectrum detection [24]. However, these methods have some disadvantages, i.e., recognition accuracy is not high enough, or the volume of the instrument is large, resulting in difficulty on many occasions. With the development of gas recognition technology, the miniaturized electronic nose [25] has attracted much attention from researchers because of its excellent portability and high recognition accuracy. However, the electronic nose system is also faced with two key problems: poor recognition ability of mixed gas signals and sensor drift caused by environmental factors, which makes it difficult to accurately identify multiple types of gas in a noisy environment. Sensor drift is usually affected by ambient temperature and humidity, gas concentration, air pressure, wind direction, and other factors. Generally speaking, sensor drift means that the measured response data will change slowly and randomly, even if the gas sensor is under the same external conditions. As time goes by, the degree of sensor drift will gradually deepen, resulting in inaccurate gas sensor data obtained in the final measurement and certain errors, which gradually reduces the accuracy of gas recognition [26]. The drift phenomenon caused by sensor measurement of gas substances seriously hinders the development of electronic nose technology; therefore, it is necessary to find a solution to sensor drift [27,28] so as to accurately identify different kinds of gas.

The main step of gas recognition of the electronic nose is the data analysis process, as shown in Figure 2. A typical data analysis process usually consists of three modules: data preprocessing, feature extraction and feature selection, and pattern recognition algorithm [29]. Among them, data preprocessing can be filtered by wavelet filter [30], Kalman filter [31], Gaussian filter [32], Savitzky–Golay filter [33], or other filtering methods, aiming to remove noise interference caused by environmental factors and sensor drift in signal data, so as to make the data more standardized. At the same time, due to the particularity of gas sensing signal data, they often have high dimensional characteristics, which can

be reduced by Principal Component Analysis [34,35] or other feature extraction [36–38] methods. Then, feature selection [39,40] is carried out from the task set and reduces the computational complexity. Finally, classical gas recognition methods, such as support vector machine [41,42], K-nearest neighbor [43], decision tree [44,45], genetic algorithm [46], and other machine learning methods, are usually applied to classify different kinds of gases. Meanwhile, experimental studies also compare the gas classification performance of different machine learning algorithms [47–49]. Classical gas identification methods generally have a relatively fixed frame and limited parameters, are easy to design, and have been widely used.

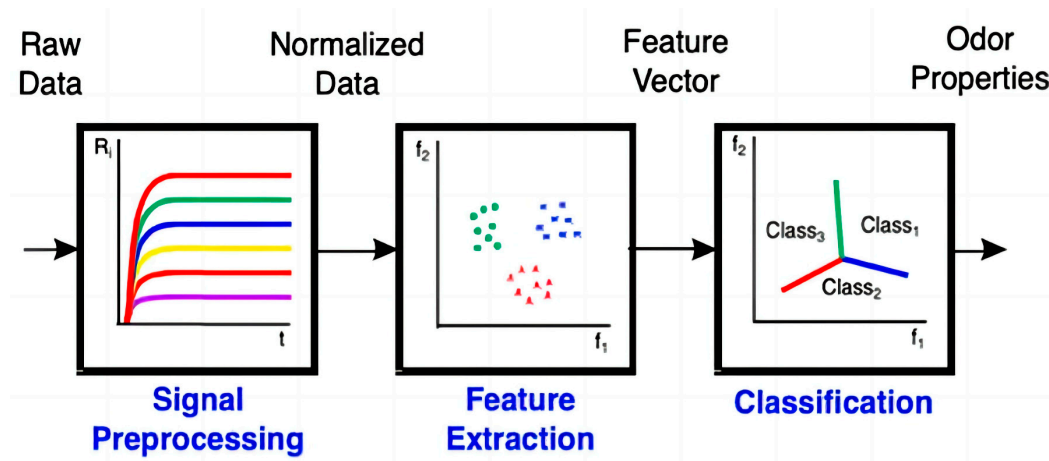


Figure 2. Data analysis in 2021 [29].

Over the years, with the development of artificial intelligence, deep learning-based gas recognition methods have been proven to be more effective for electronic noses [50–52]. Deep learning methods [53] aim to learn the internal rules and representation levels of sample data. The core idea is to realize pattern recognition of feature extraction of data through multi-layer nonlinear transformation. In deep learning, the gas recognition models shown in Figure 3 generally take the form of multi-layer neural networks. Multi-layer neural networks can distort input space and make data classes linearly separable. The task of the neural network is to minimize the value of the loss function using the gradient descent method, obtain the optimal weight parameter of each layer of neurons, and, finally, achieve convergence. The gas recognition method based on a neural network can automatically learn the deep-level gas characteristics, which greatly reduces the intervention of artificial feature extraction. The algorithm has good universality and high application value.

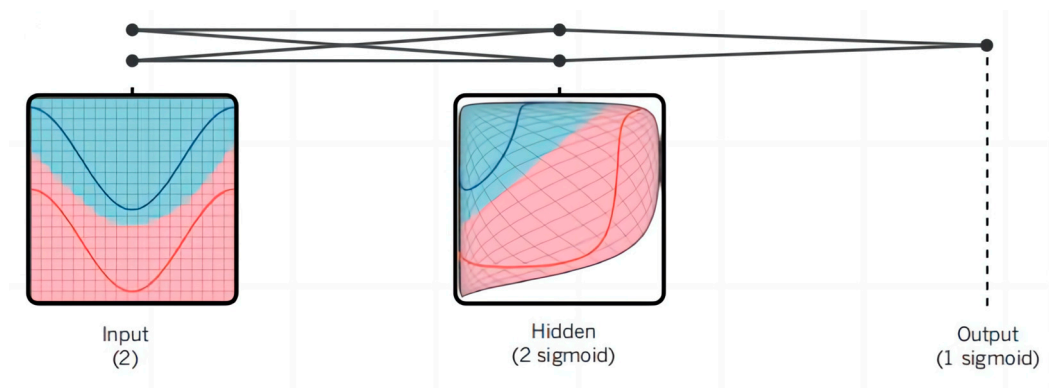


Figure 3. Schematic diagram of multi-layer neural networks in 2015 [53].

This paper reviews the typical research results of gas recognition algorithms for electronic nose systems up to now. The key points are (1) the classic gas recognition

algorithms, (2) neural network-based gas recognition algorithms, and (3) a comprehensive comparison of the performances of the above gas recognition algorithms. We hope that this review paper will provide researchers with a comprehensive overview of gas recognition algorithms for electronic nose systems.

2. Classical Gas Identification Algorithms

2.1. Classical Gas Recognition Algorithms

Over the years, a variety of classical gas recognition algorithms have been successfully applied in electronic nose systems [54]. Next, we will introduce these classical gas recognition algorithms and comprehensively compare and analyze them.

The basic working mechanism of the classical gas recognition algorithm is to design the features according to the waveform of the time series signal and discover the hidden deep structure through the features. Feature extraction of gas sensing data can obtain features with more resolution, abstractness, and invariance. Generally, the classical gas recognition algorithms mainly include the following six algorithms.

(1) Principal Component Analysis (PCA)

PCA is an unsupervised learning technique used to reduce the dimension of sample data, increase interpretability, and minimize information loss at the same time [55]. In 2008, Sen et al. used PCA to distinguish 10 kinds of gaseous hydrogen sulfide (H_2S) with different concentrations, and the recognition accuracy was 100% [56]. In 2022, Khorramifar et al. constructed an experimental electronic nose device and combined it with PCA for the identification of grape varieties [57].

PCA is mainly used to reduce the dimension of data and reduce the computational cost of the algorithm, which can remove certain noise. However, PCA is used in unsupervised and linear cases, and it cannot distinguish the electronic nose data with categories and nonlinear data. To some extent, this method limits the application of the sensor array composed of metal oxide sensors, namely the electronic nose.

(2) Linear Discriminant Analysis (LDA)

LDA is a supervised learning technique that is used to project data into a low-dimensional space and ensure that the intra-class variance of each category is small while the mean difference between classes is large [58]. In 2006, Gomez et al. used behavioral aroma information to evaluate different ripening states of tomato using PCA and LDA, as shown in Figure 4a,b. For PCA, there were obvious differences between each group and the other groups, except that the overlap degree between the half-ripe group and the unripe group was relatively light. The LDA method was adopted to classify all the different ripeness states of tomato [59]. In 2017, Choi et al. proposed an electronic nose gas classification data reconstruction method based on subspace analysis, designed an electronic nose system with stronger robustness to data errors, and enhanced the spatial discrimination ability of PCA plus LDA [60]. In 2022, Palacin et al. successfully identified complex aromas of caffeinated and decaffeinated espresso package types using LDA [61]. In the same year, Palacin et al. applied LDA to the electronic nose to classify two volatile organic compounds, ethanol and acetone [62].

In recent years, PCA and LDA, two data dimension reduction methods, have been successfully applied in gas identification to finally realize the classification and recognition of different gases. However, LDA may over-fit the data and eventually lead to a decline in gas identification accuracy.

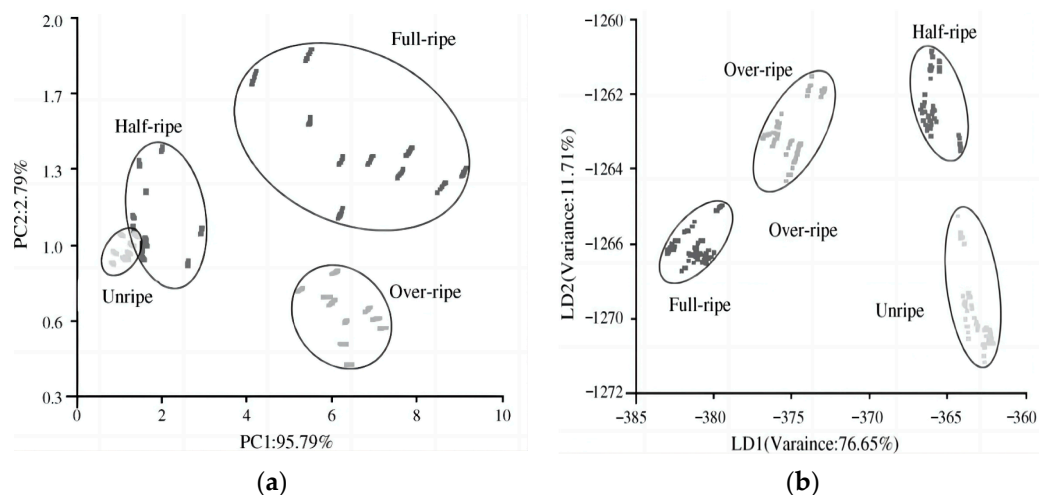


Figure 4. Results of tomato ripeness from two analysis methods: (a) PCA; (b) LDA. Reprinted with permission from Ref. [59]. Copyright year 2006, copyright owner Elsevier.

(3) Support Vector Machine (SVM)

SVM is a supervised pattern recognition and machine learning method. It is a linear classifier defined on the feature space with the largest interval, which realizes the optimization of generalization ability under the condition of limited training samples [63]. Gas recognition based on SVM is a mature theory and has been proven to be successful in many practical applications. In 2010, Pardo et al. applied SVM to the recognition of electronic nose data. In Figure 5, two separating hyperplanes are shown. The main idea of SVM is to use specific hyperplanes to separate different classes and maximize classification spacing. The interval refers to the distance from the classification hyperplane to the nearest point in the data set [64].

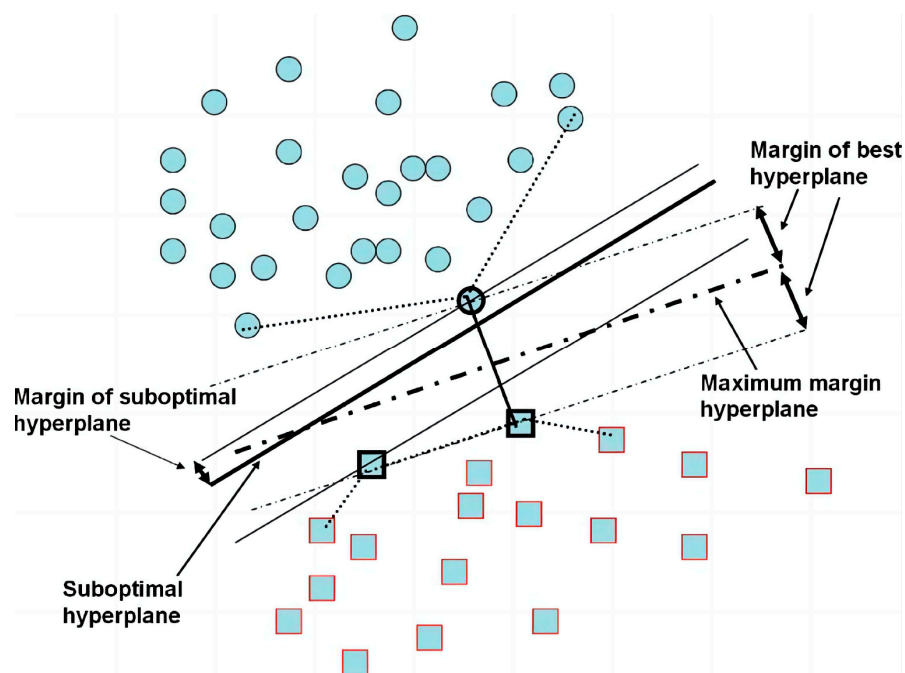


Figure 5. Two hyperplanes for the linear separable binary case. The circle and rectangle represent two different VOCs gases. Reprinted with permission from Ref. [64]. Copyright year 2005, copyright owner Elsevier.

In 2017, Qiu et al. classified gases in fruit juice food additives using the SVM method [65]. In 2021, Binston et al. applied the SVM method to the electronic nose system to detect lung cancer, chronic obstructive pulmonary disease (COPD), and other lung diseases through changes in volatile organic compounds (VOC) in exhaled gases [66]. Furthermore, some improved SVMs, for instance, the Least Squares Support Vector Machine (LSSVM), have been applied to gas identification [67,68]. In 2015, Smulko et al. successfully predicted gas concentration using a single gas sensor based on the LSSVM method. The LSSVM method does not need to remove data noise, smooth data, or other tedious data processing, which is an advantage of applying the LSSVM method to gas recognition [67]. Researchers usually adopt two or more combined algorithms for better gas classification and recognition accuracy. For example, in 2018, Chen et al. combined PCA with SVM to monitor VOC produced in the ripening process of bananas to identify different rims of bananas, with the highest recognition accuracy of 97.14% [69]. In 2019, Shi et al. combined Convolutional Neural Network (CNN) with SVM to identify beer odor information and achieved a good classification performance of 96.67% in the test set [70]. In recent years, the SVM method has been successfully applied to electronic nose systems. SVM is a novel small-sample learning method with a solid theoretical basis; therefore, it can be widely used in small-sample electronic nose data. However, the SVM method is sensitive to missing data, affecting the accuracy of gas recognition.

(4) K-Nearest Neighbor (KNN)

KNN is a supervised learning algorithm. The KNN method is widely used in non-parametric statistical methods for classification and regression due to its simplicity and remarkable classification performance [71]. In 2019, Schroeder et al. used KNN to classify several complex odors, including cheese, wine, and edible oil samples, with an identification accuracy of 91% [72]. In addition, some improved KNNs, such as Fuzzy K-Nearest Neighbor (F-KNN), are applied to gas recognition. In 2020, Mirzaee-Ghaleh et al. adopted the F-KNN algorithm to identify fresh and frozen chicken with an accuracy of 95.83% [73].

In addition, researchers often combine KNN with other algorithms to achieve better gas classification and recognition accuracy. For example, in 2018, Xu et al. used Kernel Principal Component Analysis (KPCA) to extract the characteristics of nonlinear gas mixtures of different components and combined it with KNN to recognize the target gases, with an accuracy of 98.33%. The gas recognition flow chart based on KPCA and KNN methods is shown in Figure 6. Firstly, the kernel matrix K is constructed from the training sample set. KPCA is used to extract the features of all the training samples to train the KNN classifier. Finally, the KNN algorithm is used to identify the features of test samples [74]. In 2021, Ji et al. used PCA and KNN to achieve qualitative and quantitative identification of various toxin-making chemicals, providing a new approach for rapid online detection of toxin-making chemicals sensors [4]. The KNN method can be applied to the classification of nonlinear data, and its principle is simple. However, when the data dimension is very high, the workload of computation is large. Samples that are close together may not belong to the same category.

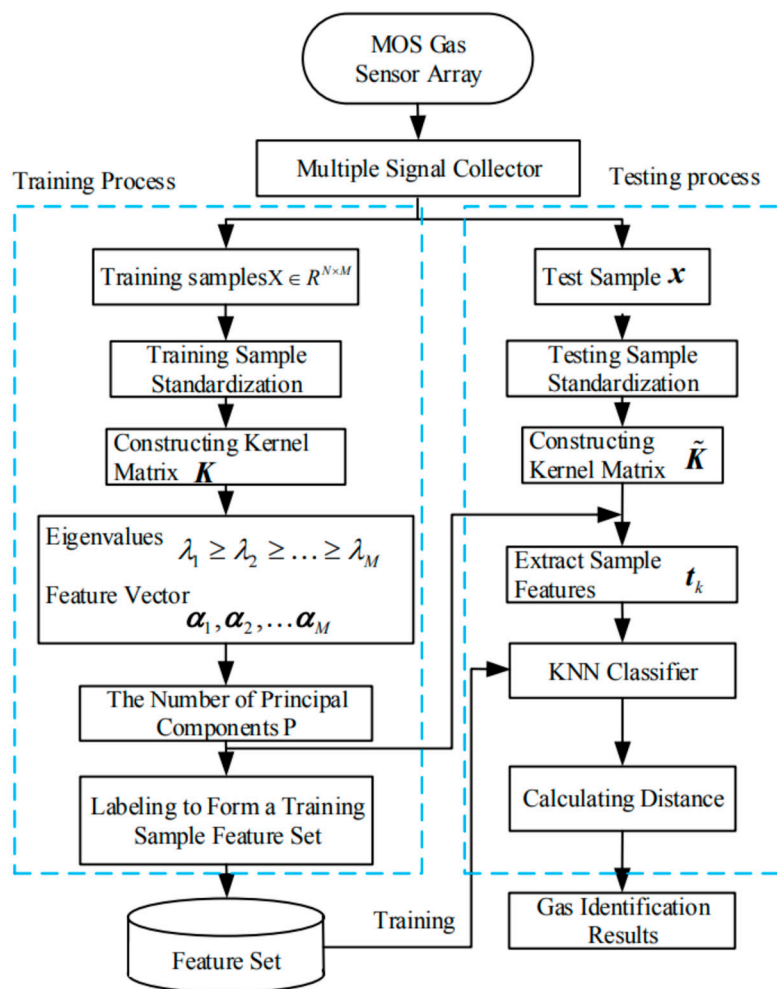


Figure 6. Flow diagram of binary mixed gas recognition method based on KPCA-KNN in 2018 [74].

(5) Decision Tree (DT)

DT is a non-parametric supervised learning method. It is a kind of decision judgment model based on a tree structure. It classifies data sets through multiple condition discrimination processes and finally obtains the required results [75]. The most important feature of a Decision Tree Classifier (DTC) is that it can decompose a complex decision judgment into a series of simpler decisions that have good explanatory ability [76]. In 2011, Cho et al. used decision tree methods of different tree models (C4.5 and CART) for the classification of electronic nose data [44]. In 2012, Cho et al. adopted a pattern recognition technique based on DT, as shown in Figure 7, to achieve the classification of explosive precursors and the estimation of their concentrations, and the recognition accuracy was 93.75% [77]. In 2014, Hassan et al. adopted the binary decision tree method for gas classification and considered the difference in sensitivity of each pair of sensors in the multi-sensor array as the input attribute of the tree. When the same concentration data were used in the training and testing stages, the accuracy of the algorithm was 100%; when different concentration data were used in the testing stage, the classification performance of the algorithm was 95.5% [78]. In 2016, He et al. used the Short-time Fourier Transform (STFT) feature extraction method combined with the DT method to classify carbon monoxide, methane, and ethanol gases of different concentrations. Considering that gas data usually contain more low-frequency information than high-frequency information, STFT is used to extract the low-frequency amplitude and is combined with a genetic algorithm to select the best features. Then, the decision tree classifier is used to achieve gas classification, and better classification results are obtained [79]. The time complexity of the DT algorithm is small and it can be used

for electronic nose data with small samples. However, over-fitting occurs easily. For data with inconsistent sample numbers in different categories, the result of DT is biased to those features with more numerical values.

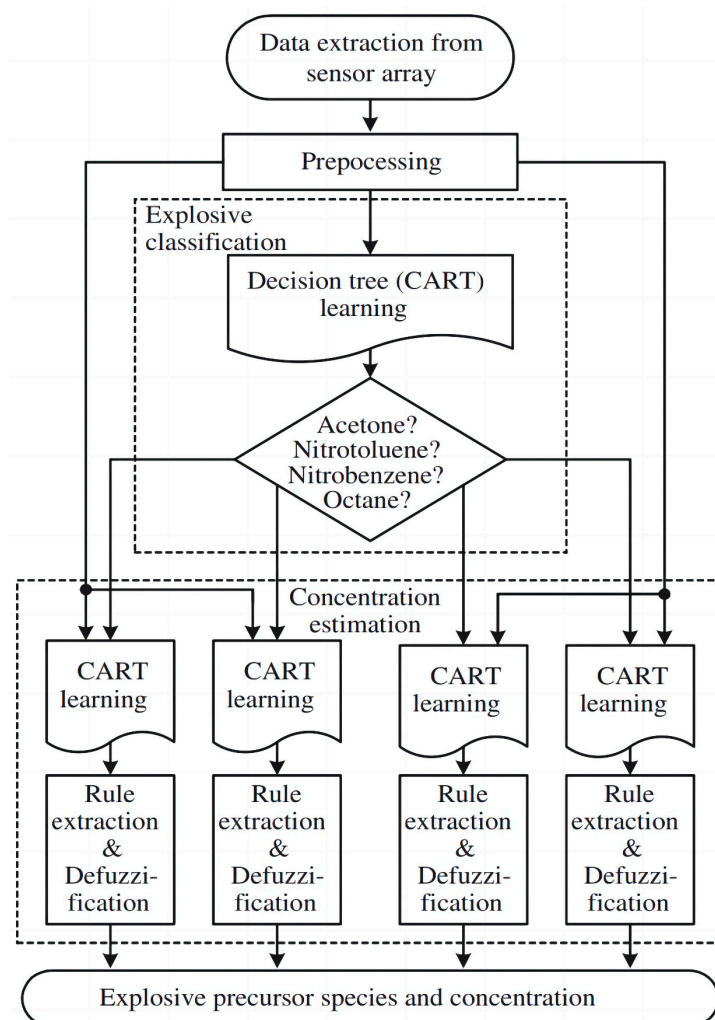


Figure 7. Flow diagram for classification and concentration estimation of explosive precursors. Reprinted with permission from Ref. [77]. Copyright year 2012, copyright owner IEEE.

(6) Random Forest (RF)

RF employs multiple decision trees to train and predict samples. That is to say, the RF algorithm contains multiple decision trees, and the category of its output is determined by the many trees of the categories of individual decision tree output [80]. In 2018, Wei et al. proposed a gas sensor array optimization method based on RF, which took Gini importance as a new measure of sensor contribution to obtain the optimal sensor array. CO, CH₄, and their mixtures were classified from an initial array of six sensors, and the recognition accuracy was 99.96% [81]. In 2020, Muhamad et al. adopted RF as a multi-classification technique to identify multiple gas by-products, eventually achieving 96.4% accuracy. As shown in Figure 8, multiple sets of data are obtained from the original training data, multiple classifiers are established, and finally, a group of classifiers is connected to build an effective combination classifier [82]. In 2022, Bogdal et al. adopted the random forest method to identify fire debris with or without gasoline, and the algorithm performed well. Compared with a convolutional neural network, the amount of training data and training time required by the random forest method are significantly less [83].

RF can handle high-dimensional and unbalanced data well, in general. However, it may not produce a good classification for small-sample data. It is more complex than the decision tree algorithm, and the calculation cost is higher.

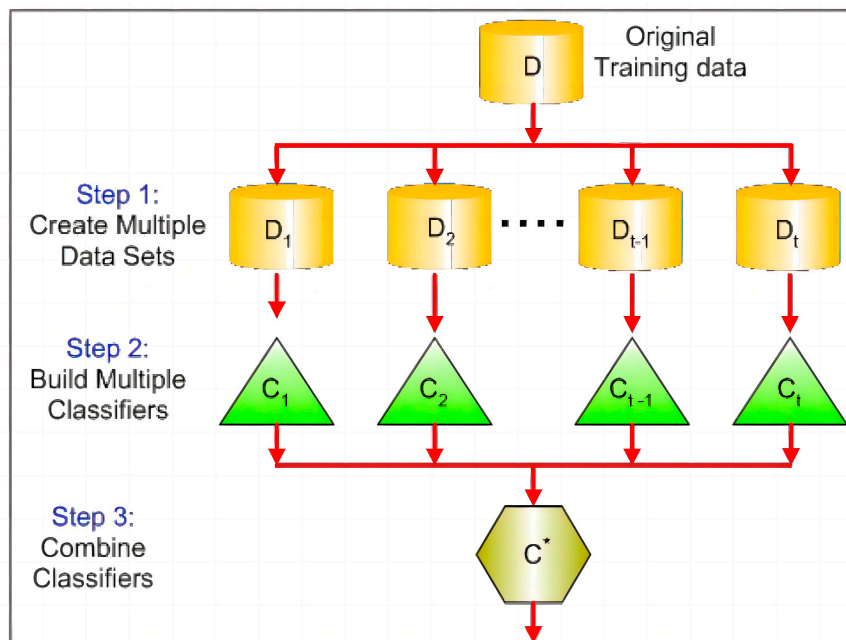


Figure 8. Flow diagram of random forest model. C^* represents the symbolic representation of the combinatorial classifier [82].

(7) Naive Bayes Model (NBM)

The Naive Bayes Model is a classification method based on Bayes' theorem and the assumption of independence of feature conditions. It is a probabilistic model with a Directed Acyclic Graph (DAG) topology that is suitable for expressing and analyzing uncertain and probabilistic events [84]. In 2017, Wijaya et al. used the Naive Bayes classifier to identify fresh beef and pork with 75% accuracy [85]. In 2019, Grodnyomchai B et al. used the Naive Bayes classifier to identify odorless, beery, whiskey, and wine flavors with 100% accuracy [86]. In 2022, Pan H et al. used the improved Naive Bayes method to identify air leaks in coal mine boreholes with an accuracy of 98.9%. As shown in Figure 9, the traditional NBM was improved using MDF theory and PCA, and the gas leakage identification model of gas extraction boreholes was established. The new classifier eliminated the shortcomings of the NBM that could not adapt to missing data and non-standard data and greatly improved the classification ability of the model [87].

The NBM algorithm is simple and easy to implement, performs well on small-sample data, and can handle multiple classification tasks. However, prior probability shall be known, and it depends on the hypothesis in many cases. The hypothesis model can have many cases; therefore, the prediction effect will be poor in some cases due to the hypothesis prior model.

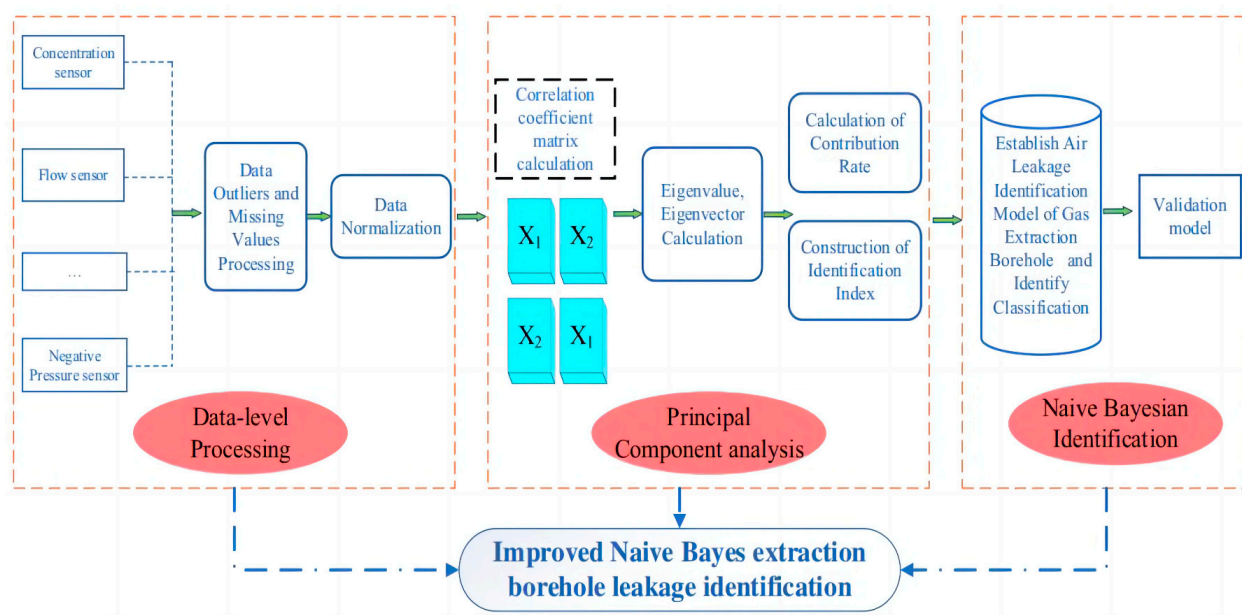


Figure 9. Flow diagram of building the model in 2022 [87].

(8) Extreme Learning Machine (ELM)

ELM is a new fast-learning algorithm, which randomly initializes the input weight, and analyzes it to determine the output weight of the network. It has few training parameters, fast learning speed, strong generalization ability, and other advantages. In 2017, Jian et al. proposed Weighted Multiple Kernel Extreme Learning Machine (QWMK-ELM) on the basis of ELM and compared it with classical classification methods, such as ELM, KELM, KNN, SVM, and MLP. Experimental results show that the proposed QWMK-ELM is superior to the above methods, not only in terms of accuracy but also in terms of gas classification efficiency [88]. In 2017, Zhang et al. combined a Self-Expression Model (SEM) and ELM to identify outliers in the electronic nose response, and a large number of experimental results have proven the effectiveness of the proposed method [89].

In 2022, Wang et al. used SVM, ELM, and Back Propagation Neural Network (BPNN) to quantitatively analyze six types of VOC. Among them, the ELM algorithm model showed the best performance; the recognition accuracy was up to 99% in the five-fold cross-validation. Figure 10 shows the schematic diagram of the integration model based on BPNN, ELM, and SVM. The integrated model has good compatibility and scalability. Using the pipeline module in sklearn, a series of data operations contained in the pattern recognition in the electronic nose system are formed into a workflow for gas recognition.

ELM is a kind of feed-forward neural network with single-layer hidden nodes, wherein the parameters of hidden nodes are randomly assigned without tuning operation, and the output weights are usually learned in one step, which makes ELM classification more efficient [90]. The hidden layer of ELM does not need iteration and has a fast learning speed and good generalization performance. However, it only considers empirical risks rather than structural risks, which may lead to the problem of over-fitting and reduce the accuracy of gas identification.

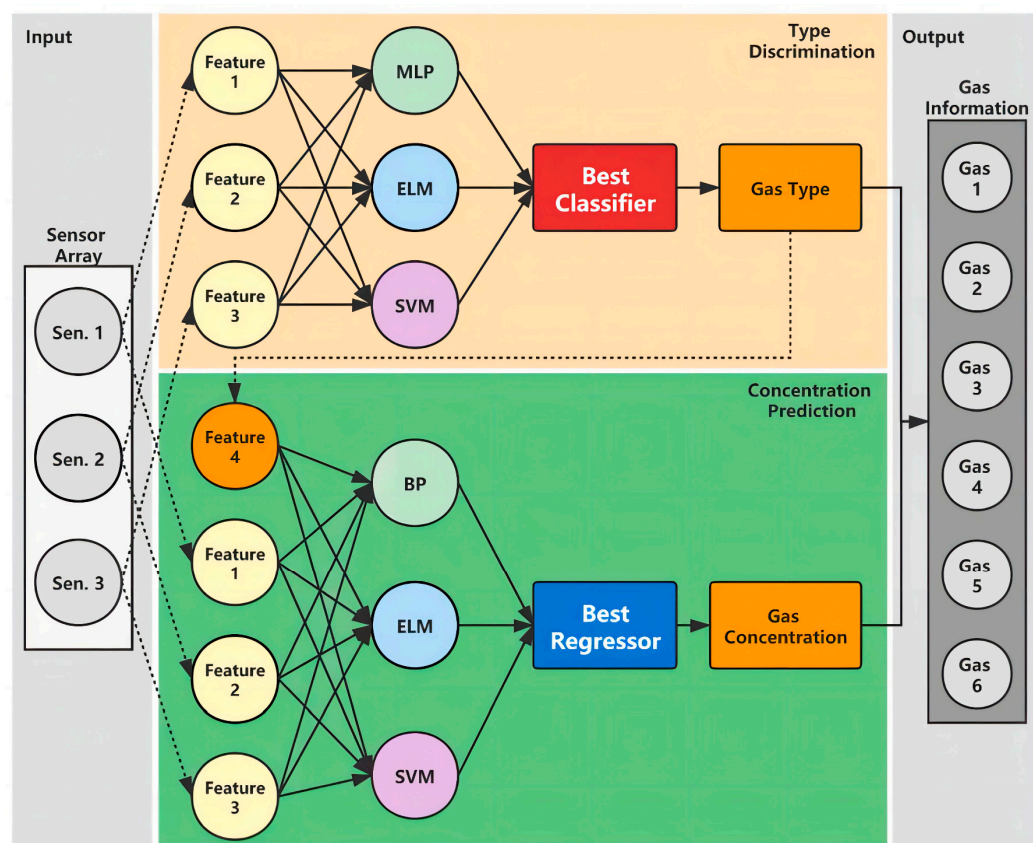


Figure 10. Schematic diagram of the integrated model, which can realize the type recognition and concentration prediction of 6 VOCs. Reprinted with permission from Ref. [90]. Copyright year 2022, copyright owner IEEE.

2.2. Analysis and Comparison of Classical Gas Recognition Algorithms

In Table 1, we summarize and compare the properties of classical gas recognition algorithms for electronic nose systems. As can be seen from Table 1, the classical gas identification algorithms generally have fast training speeds and fine interpretability, though sensitive to missing data.

It can be known from [4,56,59,74,79] that optimal gas recognition algorithms can be selected according to the characteristics of sensor signal data when carrying out gas recognition experiments. It is found from [50,67,68,73] that, in view of different gas recognition scenarios, improved classical gas recognition algorithms can achieve better gas recognition accuracy. According to [4,69,70,74,79], for specific gas recognition scenarios, the efficient combination of two or more algorithms can realize the accurate recognition of different types of gas. Many classical gas recognition algorithms, such as KNN and SVM, have relatively fixed frames and few parameters; therefore, their model generalization ability is not strong. As another example, the PCA method usually requires complex feature engineering and dimensionality reduction of data; therefore, the steps are complicated, and the application is limited. Moreover, in a complex real environment, the air humidity and temperature are often not controlled; therefore, the accuracy of the classical gas identification algorithm is greatly affected by the air temperature and humidity.

Table 1. Comparison of the classical traditional gas identification algorithms.

	PCA	LDA	SVM	KNN	DT	RF	NBM	ELM
Property	Unsupervised	Supervised	Supervised	Supervised	Supervised	Supervised	Unsupervised	Unsupervised
Training speed	Fast	Fast	Moderate	Moderate	Fast	Moderate	Moderate	Fast
Demand for data	Low	Low	Low	High	Low	High	Moderate	Low
Robustness for noise	Moderate	Moderate	Low	High	Moderate	High	Low	Low
Sensitive to missing data	Low	Low	Moderate	Low	Low	Moderate	Low	Moderate
Interpretability	Moderate	Moderate	High	High	Moderate	High	Moderate	Moderate

Since gas sensor data are usually represented as time series signals, it is necessary to artificially design features according to the waveform of time series signals [68,69]. Moreover, for classical gas recognition algorithms, the quality of feature extraction will directly affect the accuracy of final classification results, which leads to greater difficulty in feature extraction of classical gas recognition algorithms and poor algorithm universality. Research in [70–72] shows that the recognition accuracy of traditional gas recognition algorithms (for example, SVM, KNN, etc.) is lower than that of gas recognition algorithms based on neural networks (such as CNN, DCNN, etc.) for the same gas to be identified.

At the same time, because the real measurement environment of the electronic nose is very different, the change in ambient temperature and humidity will affect the response of the sensors. After investigation, the classical gas recognition algorithm cannot solve the problem of sensor drift very well.

3. Neural Network-Based Gas Recognition Algorithms

3.1. Neural Network-Based Gas Recognition Algorithms

For complex gas identification tasks, neural networks usually can perform better compared with classic ones. Compared with classical gas recognition algorithms, neural networks achieve higher gas recognition accuracy by adjusting their network layers, the number of neurons in each layer, the activation functions of neurons, and the hyperparameters, etc. Generally speaking, the more learning samples a neural network has, the stronger its generalization ability and classification recognition performance will be. Below are some progress of typical neural network-based gas recognition algorithms.

3.1.1. Back Propagation Neural Network (BPNN)

As shown in Figure 11, BPNN is a multi-layer feed-forward feedback neural network composed of an input layer, hidden layer, and output layer. By adjusting the weight between each layer, it can realize any nonlinear mapping from input to output. Moreover, the weight between each layer is optimized using the back propagation learning algorithm; therefore, it is called the back propagation neural network [91,92].

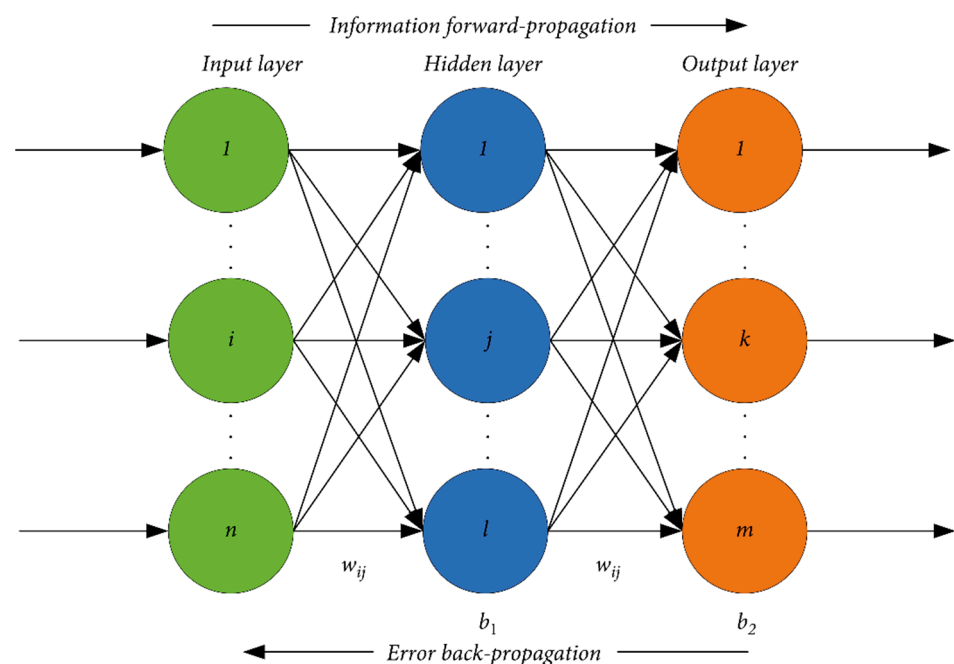


Figure 11. Back propagation neural network structure diagram in 2022 [91].

In 2013, Sunny et al. used BPNN and Average Slope Multiplication (ASM) to effectively classify different kinds of gases, and the classification accuracy was 100%. They built a

new model combining ASM and PCA algorithms to improve the BPNN algorithm. By preprocessing the data with the ASM algorithm, more effective dynamic response features can be extracted from the original response, and the quality of the data processed with ASM technology is greatly improved, giving the BPNN algorithm higher accuracy [93]. In 2019, Gu et al. used BPNN to classify and predict the species and quantity of *Aspergillus* in rice, and the recognition accuracy was 96.4% [52]. In 2021, Chu et al. adopted BPNN to recognize 11 mixture gases with an accuracy of 100% [94]. In 2013, Benrekia et al. developed an original gas recognition system for industrial gas classification. The BPNN-based classifier can effectively classify five industrial gases [95].

After carefully checking the progress of the BPNN algorithm in metal oxide sensors-based electronic noses in recent years, we conclude that, although the BPNN algorithm has an excellent performance in classification accuracy, it needs to train a large number of parameters due to its complex network structures. Therefore, it often requires a large amount of calculation when solving complex gas classification problems, resulting in long training time. In order to improve the performance of BPNN algorithms for electronic noses, it is also necessary to optimize the number of layers and parameters of the network. In most cases, combining the BPNN algorithm with other algorithms is a good route to make up for the shortcomings of the BPNN algorithm.

3.1.2. Radial Basis Function Neural Networks (RBFNN)

As shown in Figure 12, RBFNN consists of an input layer, hidden layer, and output layer. The weights between the input layer and the hidden layer are all set to 1, and the activation function of the hidden layer uses the radial basis function. The weights between the hidden layer and the output layer can be changed through training as in a normal neural network. RBFNN is a feed-forward neural network with unique best approximation, simple design, strong generalization ability, strong input noise resistance, and strong online learning ability [96]. It has been proven that RBFNN can approximate any continuous nonlinear network with any accuracy, and it is widely used in the fields of function approximation, speech recognition, pattern recognition, image processing, automatic control, and fault diagnosis.

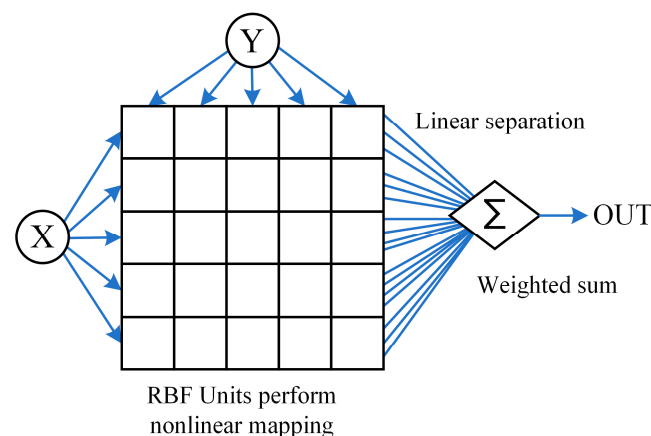


Figure 12. Structure of RBF networks.

In 2017, Jiang et al. proposed an active learning algorithm that effectively combined Query By Committee (QBC) and RBFNN into the electronic nose, achieving good classification and recognition accuracy of indoor pollutants such as toluene, formaldehyde, and benzene [97]. In 2018, Zhang et al. proposed an oil and gas pipeline defect recognition model based on the RBFNN model and adopted the Improved Particle Swarm Optimization algorithm (IPSO-RBFNN) to select the optimal parameters, finally achieving a higher recognition accuracy. The model adopts entropy-based population initialization, uses dynamically adjusted inertia weight and improved learning factor to improve PSO,

and effectively solves the problems of traditional IPSO, such as long search time and easy-to-capture local minimum [98].

Considering the application of the RBFNN algorithm in the electronic nose, it effectively avoids the local optimum problem of the BPNN algorithm, and its strong robustness and online learning ability can also improve the performance of the electronic nose. However, RBFNN and BPNN algorithms share the same shortcomings. They require a large amount of data to complete the training of network parameters; therefore, optimizing the network model and completing the training with fewer data and faster time becomes particularly important.

3.1.3. Convolutional Neural Network (CNN)

CNN is widely used in the field of image recognition, and it is inspired by the natural visual perception mechanism of biology. As shown in Figure 13, it is usually composed of one or more convolution layers, pooling layers, and fully connected layers. Peng et al. first applied CNN to gas identification in 2018. They designed a Deep Convolutional Neural Network (DCNN) with up to 38 layers that identified four different odors with 95.2% accuracy [99]. In 2019, Pan et al. proposed a new method combining hybrid CNN and Recurrent Neural Network (RNN) to quickly identify four different gases, with the highest accuracy of 98.28% [100].

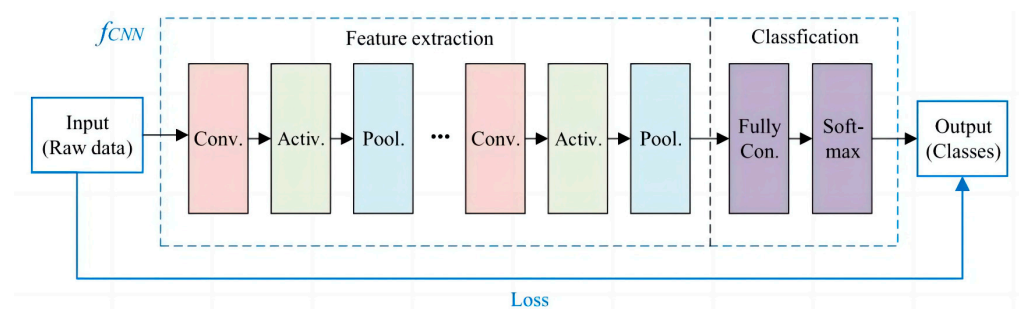


Figure 13. The framework of the CNN-based model in 2022. Reprinted with permission from Ref. [101]. Copyright year 2023, copyright owner IEEE.

In 2020, Wang et al. proposed an optimized DCNN, which uses a special strip 1D kernel in the convolutional layer and pooling layer, as shown in Figure 14, and has an accuracy rate of 87.56% for the classification of various Chinese herbal medicines [102].

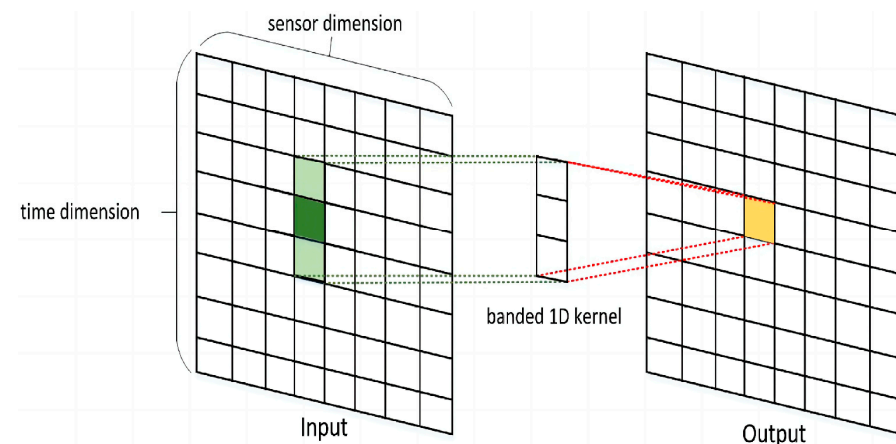


Figure 14. An illustration of the banded 1D convolution kernel in deep CNN. Reprinted with permission from Ref. [59]. Copyright year 2020, copyright owner Elsevier.

In 2021, Ma et al. proposed a new method combining a dynamic response graph with a Deep Learning Model (DLM), and the recognition accuracy of 10 VOCs was 92% [103]. In 2021, Xiong et al. combined CNN with Spiking Neuron Networks (SNN) to identify the mixed odor of spoiled food and rotten fruit, with an average test accuracy of 84.5% and 88.6%, respectively [104]. In 2022, Zhao et al. proposed a new One-Dimensional Deep Convolutional Neural Network (1D-DCNN). This method has an algorithm based on a multi-label method, which can fully and automatically extract and classify the features of a gas mixture with an accuracy of 96.3% [105].

In 2022, Sharma et al. designed an effective and reliable gas hazard monitoring system by combining a filter based on Dempster–Shafer Evidence Theory (DSET) with a One-Dimensional Convolutional Neural Network (1DCNN) classifier, which solved a problem in underground coal mines and mining operations. However, the accuracy of gas classification may be affected by the failure of gas sensors due to the harsh environment. By fusing DSET and 1DCNN, the classification accuracy reached 99.6%, even in the case of partial sensor failure [106]. In 2022, Feng et al. proposed Augmented Convolutional Neural Network (ACNN). The ACNN model is a constantly updated machine-learning framework that automatically converts time-varying gas signals into multidimensional characteristic matrices. Then, the knowledge of the existing model is extended with the incremental data through internal parameter tuning, and the model deviation is further compensated with an external adjustment module on the basic CNN classifier. Finally, the pattern recognition method can solve the problem of gas identification for a long time with high accuracy, and it can deal with the sensor drift problem well [101]. In 2022, Sun et al. combined the gas sensor array with the CNN pattern recognition model to identify the freshness of refrigerated tilapia, with an accuracy of 92.31% [107].

It can be seen that the CNN algorithm can automatically extract data features and has a better application effect in the metal oxide sensor array. Both in terms of classification accuracy and training speed, the CNN algorithm has more advantages than the traditional machine learning and BP neural network. At the same time, as mentioned in article [105], the CNN algorithm can also maintain a very high accuracy under strong interference. However, when using a gradient descent algorithm to train CNN, the training results are easy to converge to the local minimum rather than the global minimum, and the selection of pooling layer parameters will also directly affect the final classification accuracy. Therefore, to improve the performance of the metal oxides-based electronic nose, the CNN algorithm should adopt more efficient trainers or be combined with other algorithms, automatically extracting more valuable features from small data.

3.1.4. Recurrent Neural Network (RNN)

On the basis of traditional neural networks, RNN introduces state variables to store past information and set weights and output results together with the current input. This optimization allows RNN to handle timing information better. Although RNN can deal with certain short-term dependencies, it cannot deal with long-term dependencies. When the sequence is long, it is difficult for the gradient at the back of the sequence to propagate back to the previous sequence, which leads to the problem of gradient disappearance. In order to improve the computing efficiency of RNN and avoid gradient disappearance, Hochreiter and Schmidhuber proposed Long Short-Term Memory (LSTM) in 1997. Its structure is shown in Figure 15. By adding an input gate, forgetting gate, and output gate, a sigmoid function was introduced and combined with the tanh function. The possibility of gradient vanishing and gradient explosion is effectively reduced [108].

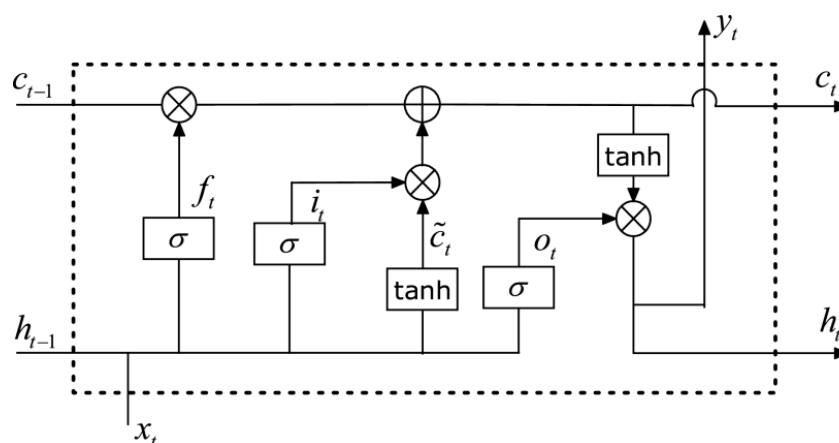


Figure 15. The LSTM cell structure diagram. Reprinted with permission from Ref. [109]. Copyright year 2021, copyright owner IEEE.

In 2019, Wang et al. proposed a cyclic neural network based on LSTM to solve the problem of chemical sensor drift. This technology can better mine the deep information of sensor drift signals, replace manual extraction, and more accurately match complex nonlinearity. The proposed LSTM prediction model can predict the baseline and drift of chemical sensors in the long term and accurately [110]. In 2021, Zou et al. used RNN to classify six gases, with an average accuracy of 95% [111]. In 2021, Zhang et al. proposed a new gas recognition and concentration estimation model based on a many-to-many long short-term memory-recurrent neural network (LSTM-RNN) and dynamic wavelet convolutional neural network and realized the recognition of carbon monoxide, hydrogen gas, and carbon monoxide and hydrogen gas mixture with accuracy close to 100% [109]. In 2021, Kwon et al. proposed a gas detection system based on RNN and prepared a gas sensor for detecting nitrogen dioxide and hydrogen sulfide using In_2O_3 films as sensing materials. The RNN algorithm mentioned in this paper has better gas classification accuracy than other algorithms, even when using fewer input neurons and smaller arrays, which makes the RNN algorithm with small arrays more suitable for low-power metal oxide sensors [112]. In 2021, Bakiler et al. used the method of LSTM-RNN to extract the features of gas data signals, realizing the classification of carbon monoxide, ethylene, ethanol, and methane with the highest accuracy of 90.8%. Compared with other traditional pattern recognition methods, the accuracy has been greatly improved [113].

The RNN algorithm correlates the information of time series by adding memory units. This feature allows the RNN algorithm to use fewer data and extract more effective features; therefore, the RNN algorithm is widely used in fast gas identification. However, it should be noted that the problem of gradient disappearance easily occurs when using the RNN algorithm, resulting in a poor model training effect.

3.1.5. Spiking Neural Network (SNN)

SNN is a new generation artificial neural network model derived from biological inspiration, which is the most reasonable neuronal model in biology. It is used to capture the observed information dynamics among real biological neurons and represent and integrate multiple information dimensions [114]. As shown in Figure 16, different from classical neural networks, neurons in pulsed neural networks are not activated in every iteration propagation but only when their membrane potential reaches a certain threshold.

The model structure is shown in Figure 17. This structure mimics the basic structure of the mammalian olfactory system. The network consists of three layers: the olfactory neuron layer, the mitral valve cell layer, and the granular cell layer. The olfactory neuron layer converts chemical information about odors into electrical information and sends this information to the mitral valve cell layer. The mitral valve cell layer and granulososa cell layer perform signal processing and initial odor recognition. The granulososa layer is an inhibitory

cell that helps modify signaling and sorting. The connections between different olfactory neuron layers are considered to be transverse connections, while the connections between olfactory neuron layers and mitral valve cell layers are considered to be feed-forward connections [115].

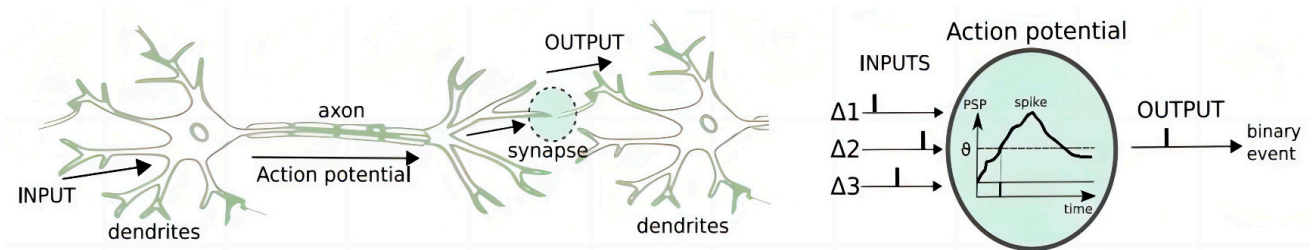


Figure 16. Biological neuron and its association with an artificial spiking neuron. Reprinted with permission from Ref. [114]. Copyright year 2020, copyright owner Elsevier.

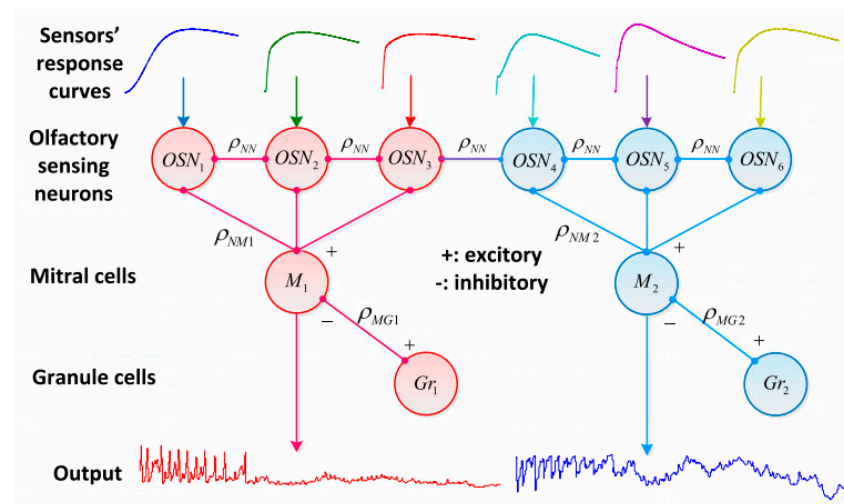


Figure 17. Structure of the proposed olfactory neural network. Reprinted with permission from Ref. [115]. Copyright year 2016, copyright owner IEEE.

In 2015, Sankho et al. applied SNN to the odor classification of orthodox black tea with the highest accuracy of 94.68% [116]. In 2016, Jing et al. combined SNN and SVM to classify seven kinds of liquor with an accuracy rate of 93%, which was an obvious improvement compared with that of LDA/SVM/BPNN, three traditional pattern recognition algorithms [115]. In 2022, Han et al. used SNN to analyze complex mixed signals to identify odor sources, and the classification accuracy reached 98.25%. Meanwhile, SNN has achieved a good energy-saving effect compared with a traditional electronic nose using deep neural network algorithms [117]. In 2021, Kwon et al. proposed an artificial olfactory system based on SNN and field effect transistors-type gas sensors to realize rapid and reliable detection of toxic gases. Only the first 5 s of response data from 12 sensors were used, and the error rate of SNN in predicting nitrogen dioxide and hydrogen sulfide concentrations was less than 3% [118].

Considering the use of the SNN algorithm for metal oxide sensors, we conclude that the SNN algorithm has stronger robustness in that gas data can be easily affected by temperature, humidity, and other environmental effects, and the SNN algorithm can deal with the data drift problem of metal oxide sensors well. However, since the framework of SNN algorithms is not yet perfect, SNN for gas identification has many challenges in terms of accuracy and design complexity.

3.2. Analysis and Comparison of Gas Recognition Algorithms Based on Neural Network

In Table 2, we summarize and compare the gas recognition algorithms based on neural networks. From Table 2, it can be found that RBFNN, CNN, and SNN have faster training speeds, and CNN, RNN, and SNN have stronger noise robustness. Generally speaking, with enough training samples, the gas recognition algorithm based on a neural network usually has higher gas recognition accuracy than the classical one. The algorithms can be optimized by adjusting their network layers, the number of neurons in each layer, the activation function of neurons, and hyper-parameters so as to achieve higher gas recognition accuracy.

Table 2. Comparison based on neural network gas identification algorithms.

	BPNN	RBFNN	CNN	RNN	SNN
Property	Unsupervised	Supervised	Supervised	Supervised	Unsupervised/Supervised
Training speed	Slow	Fast	Fast	Moderate	Fast
Demand for data	Moderate	Moderate	High	Low	High
Robustness for noise	Moderate	Moderate	High	High	High
Sensitive to missing data	Low	Low	Low	Low	Low
Interpretability	High	Moderate	Moderate	Moderate	Moderate

It is found from the studies in [93,94,101,104] that neural networks such as BPNN, CNN, RNN, SNN, RBFNN, etc., have advantages in gas recognition accuracy and the number of gas types. One critical reason is that when the data size is large enough, the classical gas recognition algorithms will encounter a recognition performance bottleneck in the case of limited parameters and a relatively fixed frame, but the gas recognition accuracy based on neural networks can be further improved. At the same time, the accuracy of the classical gas recognition algorithms depends very much on the quality of feature extraction of data. It is found that the classical gas recognition algorithms can achieve good accuracy under the limited small sample types. However, with the increase in gas recognition types, the accuracy of the classical gas recognition algorithm declines. When more than five kinds of gas are identified, the classical gas recognition algorithm cannot give good classification results. However, the neural network-based gas recognition algorithms also have good accuracy when more than 10 kinds of gas are classified. Because the neural network algorithms have stronger learning ability, i.e., they usually have enough sample data to train the neural network, gas recognition can achieve higher classification accuracy.

At the same time, neural network-based gas recognition algorithms can achieve higher classification accuracy and faster training speed by selecting proper optimizers when training the network. Classical optimizers in the past include the Stochastic Gradient Descent (SGD) method, which randomly selects one sample each time. Although it enables the parameter updating speed to reach the optimal value more quickly, the frequent updating of the SGD method sometimes causes serious shock to the loss function. In recent years, with the continuous development of deep learning, more and more excellent optimizers have been designed, among which Adaptive Moment Estimation (Adam) has the advantages of simple implementation, efficient calculation, and few memory requirements. At the same time, the learning rate can be automatically adjusted during the training process. The emergence of the Adam optimizer makes the training of the model more efficient. In [110], the author successfully applied the Adam optimizer in the deep convolutional neural network of the training electronic nose, making the whole training process of the model more efficient.

4. Conclusions

This paper reviews the gas recognition methods in metal oxide-based electronic noses, including the classical and neural network-based algorithms, and analyzes and compares the performance of different gas recognition algorithms. It is found that the classical gas recognition algorithms are simple to implement and have obvious advantages in classifying small-sample data. However, classical gas recognition algorithms usually require complex

feature engineering, which requires dimensionality reduction, feature extraction and feature selection of data, etc.; therefore, the steps are complicated, and the application is limited. In contrast, neural network-based gas recognition algorithms usually have higher gas recognition accuracy than classical ones. Neural network-based gas recognition algorithms can be optimized by adjusting their network layer structures, the number of neurons in each layer, and the activation function of neurons and hyperparameters to achieve higher gas recognition accuracy. At the same time, the gas recognition model based on a neural network has better anti-interference ability and stronger robustness.

In the future, a lighter and more efficient gas recognition model will be constructed and applied to different scenarios to realize the wide application of metal oxides-based electronic nose systems.

Author Contributions: Conceptualization, M.J.; methodology, Z.Z.; software, X.W.; validation, X.W., Y.Z., and M.J.; formal analysis, Z.Z.; investigation, X.F.; resources, M.J.; data curation, X.W.; writing—original draft preparation, X.W. and Y.Z.; writing—review and editing, M.J.; visualization, X.W. and Y.Z.; supervision, M.J.; project administration, Z.Z.; funding acquisition, Z.W. and M.J. All authors have read and agreed to the published version of the manuscript.

Funding: This research was funded by the Ministry of Science and Technology of China (2022CSJGG0703), National Natural Science Foundation of China (62204260, 52204253), Opening Foundation of Civil Aircraft Fire Science and Safety Engineering Key Laboratory of Sichuan Province (MZ2023KF06).

Institutional Review Board Statement: Not applicable.

Informed Consent Statement: Not applicable.

Data Availability Statement: No new data were created or analyzed in this study. Data sharing is not applicable to this article.

Conflicts of Interest: The authors declare no conflict of interest.

References

1. Persaud, K.; Dodd, G. Analysis of discrimination mechanisms in the mammalian olfactory system using a model nose. *Nature* **1982**, *299*, 352–355. [[CrossRef](#)] [[PubMed](#)]
2. Liu, H.; Meng, G.; Deng, Z.; Li, M.; Chang, J.; Dai, T.; Fang, X. Progress in Research on VOC Molecule Recognition by Semiconductor Sensors. *Acta Phys. Chim. Sin.* **2022**, *38*, 2008018. [[CrossRef](#)]
3. Meng, F.; Li, X.; Yuan, Z.; Lei, Y.; Qi, T.; Li, J. Ppb-Level Xylene Gas Sensors based on Co₃O₄ Nanoparticles coated Reduced Graphene Oxide (rGO) Nanosheets Operating at Low Temperature. *IEEE Trans. Instrum. Meas.* **2021**, *70*, 9511510. [[CrossRef](#)]
4. Ji, H.; Qin, W.; Yuan, Z.; Meng, F. Qualitative and quantitative recognition method of drug-producing chemicals based on SnO₂ gas Sensor with dynamic measurement and PCA weak separation. *Sens. Actuators B Chem.* **2021**, *348*, 130698.
5. Qin, W.; Yuan, Z.; Gao, H.; Zhang, R.; Meng, F. Perovskite-structured LaCoO₃ modified ZnO gas sensor and investigation on its gas sensing mechanism by first principle. *Sens. Actuators B Chem.* **2021**, *341*, 130015.
6. Meng, F.; Shi, X.; Yuan, Z.; Ji, H.; Qin, W.; Shen, Y.; Xing, C. Detection of Four Alcohol Homologue Gases by ZnO Gas Sensor in Dynamic Interval Temperature Modulation Mode. *Sens. Actuators B Chem.* **2022**, *350*, 130867. [[CrossRef](#)]
7. Meng, F.; Qi, T.; Zhang, J.; Zhu, H.; Yuan, Z.; Liu, C.; Qin, W.; Ding, M. MoS₂-templated porous hollow MoO₃ microspheres for highly selective ammonia sensing via a Lewis acid-base interaction. *IEEE Trans. Ind. Electron.* **2022**, *69*, 960–970. [[CrossRef](#)]
8. Jiao, M.; Chen, X.; Hu, K.; Qian, D.; Zhao, X.; Ding, E. Recent developments of nanomaterials-based conductive type methane sensors. *Rare Met.* **2021**, *40*, 1515–1527.
9. Navaneeth, B.; Suchetha, M. PSO optimized 1-D CNN-SVM architecture for real-time detection and classification applications. *Comput. Biol. Med.* **2019**, *108*, 85–92. [[CrossRef](#)]
10. Guntner, A.T.; Abegg, S.; Konigstein, K.; Gerber, P.A.; Schmidt-Trucksass, A.; Pratsinis, S.E. Breath sensors for health monitoring. *ACS Sens.* **2019**, *4*, 268–280.
11. Das, S.; Pal, M. Non-invasive monitoring of human health by exhaled breath analysis: A comprehensive review. *J. Electrochem. Soc.* **2020**, *167*, 037562. [[CrossRef](#)]
12. Tai, H.; Wang, S.; Duan, Z.; Jiang, Y. Evolution of breath analysis based on humidity and gas sensors: Potential and challenges. *Sens. Actuators B Chem.* **2020**, *318*, 128104. [[CrossRef](#)]
13. Paleczek, A.; Rydosz, A. Review of the algorithms used in exhaled breath analysis for the detection of diabetes. *J. Breath Res.* **2022**, *16*, 026003. [[CrossRef](#)]
14. Paknahad, M.; Ahmadi, A.; Rousseau, J.; Nejad, H.R.; Hoorfar, M. On-chip electronic nose for wine tasting: A digital microfluidic approach. *IEEE Sens. J.* **2017**, *17*, 4322–4329. [[CrossRef](#)]

15. Hidayat, S.N.; Triyana, K.; Fauzan, I.; Julian, T.; Lelono, D.; Yusuf, Y.; Ngadiman, N.; Vesolo, A.C.A.; Peres, A.M. The electronic nose coupled with chemometric tools for discriminating the quality of black tea samples in situ. *Chemosensors* **2019**, *7*, 29. [[CrossRef](#)]
16. Pulluri, K.K.; Kumar, V.N. Development of an Integrated Soft E-nose for Food Quality Assessment. *IEEE Sens. J.* **2022**, *22*, 15111–15122. [[CrossRef](#)]
17. Lamagna, A.; Reich, S.; Rodríguez, D.; Boselli, A.; Cicerone, D. The use of an electronic nose to characterize emissions from a highly polluted river. *Sens. Actuators B Chem.* **2008**, *131*, 121–124. [[CrossRef](#)]
18. Ma, H.; Wang, T.; Li, B.; Cao, W.; Zeng, M.; Yang, J.; Su, Y.; Hu, N.; Zhou, Z.; Yang, Z. A low-cost and efficient electronic nose system for quantification of multiple indoor air contaminants utilizing HC and PLSR. *Sens. Actuators B Chem.* **2022**, *350*, 130768. [[CrossRef](#)]
19. Liu, M.; Li, Y. Application of electronic nose technology in coal mine risk prediction. *Chem. Eng. Trans.* **2018**, *68*, 307–312.
20. Comito, C.; Pizzuti, C. Artificial intelligence for forecasting and diagnosing COVID-19 pandemic: A focused review. *Artif. Intell. Med.* **2022**, *128*, 102286. [[CrossRef](#)]
21. Hidayat, S.N.; Julian, T.; Dharmawan, A.B.; Puspita, M.; Chandra, L.; Rohman, A.; Julia, M.; Rianjanu, A.; Nurputra, D.K.; Triyana, K.; et al. Hybrid learning method based on feature clustering and scoring for enhanced COVID-19 breath analysis by an electronic nose. *Artif. Intell. Med.* **2022**, *129*, 102323. [[CrossRef](#)] [[PubMed](#)]
22. Nurputra, D.K.; Kusumaatmaja, A.; Hakim, M.S.; Hidayat, S.N.; Julian, T.; Sumanto, B.; Mahendradhata, Y.; Saktiawati, A.M.; Wasisto, H.S.; Triyana, K. Fast and noninvasive electronic nose for sniffing out COVID-19 based on exhaled breath-print recognition. *NPJ Digit. Med.* **2022**, *5*, 115. [[CrossRef](#)] [[PubMed](#)]
23. Mendis, S.; Sobotka, P.A.; Euler, D.E. Pentane and isoprene in expired air from humans: Gas-chromatographic analysis of single breath. *Clin. Chem.* **1994**, *40*, 1485–1488. [[CrossRef](#)] [[PubMed](#)]
24. Wang, C.; Sahay, P. Breath analysis using laser spectroscopic techniques: Breath biomarkers, spectral fingerprints, and detection limits. *Sensors* **2009**, *9*, 8230–8262. [[CrossRef](#)]
25. Arroyo, P.; Meléndez, F.; Suárez, J.I.; Herrero, J.L.; Rodríguez, S.; Lozano, J. Electronic nose with digital gas sensors connected via bluetooth to a smartphone for air quality measurements. *Sensors* **2020**, *20*, 786. [[CrossRef](#)]
26. Romain, A.C.; André, P.; Nicolas, J. Three years experiment with the same tin oxide sensor arrays for the identification of malodorous sources in the environment. *Sens. Actuators B Chem.* **2002**, *84*, 271–277. [[CrossRef](#)]
27. Liu, Q.; Li, X.; Ye, M.; Ge, S.S.; Du, X. Drift compensation for electronic nose by semi-supervised domain adaption. *IEEE Sens. J.* **2013**, *14*, 657–665. [[CrossRef](#)]
28. Zhang, L.; Zhang, D. Domain adaptation extreme learning machines for drift compensation in E-nose systems. *IEEE Trans. Instrum. Meas.* **2014**, *64*, 1790–1801. [[CrossRef](#)]
29. Covington, J.A.; Marco, S.; Persaud, K.C.; Schiffman, S.S.; Troy Nagle, H. Artificial Olfaction in the 21st Century. *IEEE Sens. J.* **2021**, *21*, 12969–12990. [[CrossRef](#)]
30. Donoho, D.L.; Johnstone, J.M. Ideal spatial adaptation by wavelet shrinkage. *Biometrika* **1994**, *81*, 425–455. [[CrossRef](#)]
31. Auger, F.; Hilairt, M.; Guerrero, J.M.; Monmasson, E.; Orłowska-Kowalska, T.; Katsura, S. Industrial applications of the Kalman filter: A review. *IEEE Trans. Ind. Electron.* **2013**, *60*, 5458–5471. [[CrossRef](#)]
32. Afshari, H.H.; Gadsden, S.A.; Habibi, S. Gaussian filters for parameter and state estimation: A general review of theory and recent trends. *Signal Process.* **2017**, *135*, 218–238. [[CrossRef](#)]
33. Wang, X.; Qian, C.; Zhao, Z.; Li, J.; Jiao, M. A Novel Gas Recognition Algorithm for Gas Sensor Array Combining Savitzky–Golay Smooth and Image Conversion Route. *Chemosensors* **2023**, *11*, 96. [[CrossRef](#)]
34. Schreyer, S.K.; Mikkelsen, S.R. Chemometric analysis of square wave voltammograms for classification and quantitation of untreated beverage samples. *Sens. Actuators B Chem.* **2000**, *71*, 147–153. [[CrossRef](#)]
35. Abdi, H.; Williams, L.J. Principal component analysis. *Wiley Interdiscip. Rev. Comput. Stat.* **2010**, *2*, 433–459. [[CrossRef](#)]
36. Liu, T.; Zhang, W.; Ye, L.; Ueland, M.; Forbes, S.L.; Su, S.W. A novel multi-odour identification by electronic nose using non-parametric modelling-based feature extraction and time-series classification. *Sens. Actuators B Chem.* **2019**, *298*, 126690. [[CrossRef](#)]
37. Jong, G.J.; Hendrick; Wang, Z.; Hsieh, K.S.; Horng, G.J. A novel feature extraction method an electronic nose for aroma classification. *IEEE Sens. J.* **2019**, *19*, 10796–10803. [[CrossRef](#)]
38. Liu, T.; Zhang, W.; Li, J.; Ueland, M.; Forbes, S.L.; Zheng, W.; Su, S.W. A Multiscale Wavelet Kernel Regularization-Based Feature Extraction Method for Electronic Nose. *IEEE Trans. Syst. Man Cybern. Syst.* **2022**, *52*, 7078–7089. [[CrossRef](#)]
39. Wijaya, D.R.; Afianti, F. Information-theoretic ensemble feature selection with multi-stage aggregation for sensor array optimization. *IEEE Sens. J.* **2021**, *21*, 476–489. [[CrossRef](#)]
40. Attallah, O.; Morsi, I. An electronic nose for identifying multiple combustible/harmful gases and their concentration levels via artificial intelligence. *Measurement* **2022**, *199*, 111458. [[CrossRef](#)]
41. Ge, H.; Liu, J. Identification of gas mixtures by a distributed support vector machine network and wavelet decomposition from temperature modulated semiconductor gas sensor. *Sens. Actuators B Chem.* **2006**, *117*, 408–414. [[CrossRef](#)]
42. Brudzewski, K.; Osowski, S.; Markiewicz, T. Classification of milk by means of an electronic nose and SVM neural network. *Sens. Actuators B Chem.* **2004**, *98*, 291–298. [[CrossRef](#)]

43. Martin, Y.G.; Oliveros, M.C.C.; Pavón, J.L.P. Electronic nose based on metal oxide semiconductor sensors and pattern recognition techniques: Characterisation of vegetable oils. *Anal. Chim. Acta* **2001**, *449*, 69–80. [[CrossRef](#)]
44. Cho, J.H.; Kurup, P.U. Decision tree approach for classification and dimensionality reduction of electronic nose data. *Sens. Actuators B Chem.* **2011**, *160*, 542–548. [[CrossRef](#)]
45. Li, Q.; Bermak, A. A low-power hardware-friendly binary decision tree classifier for gas identification. *J. Low Power Electron. Appl.* **2011**, *1*, 45–58. [[CrossRef](#)]
46. Gardner, J.W.; Boilot, P.; Hines, E.L. Enhancing electronic nose performance by sensor selection using a new integer-based genetic algorithm approach. *Sens. Actuators B Chem.* **2005**, *106*, 114–121. [[CrossRef](#)]
47. Gromski, P.S.; Correa, E.; Vaughan, A.A.; Wedge, D.C.; Turner, M.L.; Goodacre, R. A comparison of different chemometrics approaches for the robust classification of electronic nose data. *Anal. Bioanal. Chem.* **2014**, *406*, 7581–7590. [[CrossRef](#)]
48. Xu, L.; He, J.; Duan, S.; Wu, X.; Wang, Q. Comparison of machine learning algorithms for concentration detection and prediction of formaldehyde based on electronic nose. *Sens. Rev.* **2016**, *36*, 207–216. [[CrossRef](#)]
49. De Vito, S.; Esposito, E.; Salvato, M.; Popoola, O.; Formisano, F.; Jones, R.; Francia, G.D. Calibrating chemical multisensory devices for real world applications: An in-depth comparison of quantitative machine learning approaches. *Sens. Actuators B Chem.* **2018**, *255*, 1191–1210. [[CrossRef](#)]
50. Yu, H.; Wang, J.; Xiao, H.; Liu, M. Quality grade identification of green tea using the eigenvalues of PCA based on the E-nose signals. *Sens. Actuators B Chem.* **2009**, *140*, 378–382. [[CrossRef](#)]
51. Timsorn, K.; Thoopboochagorn, T.; Lertwattanasakul, N.; Wongchoosuk, C. Evaluation of bacterial population on chicken meats using a briefcase electronic nose. *Biosyst. Eng.* **2016**, *151*, 116–125. [[CrossRef](#)]
52. Gu, S.; Wang, J.; Wang, Y. Early discrimination and growth tracking of *Aspergillus* spp. contamination in rice kernels using electronic nose. *Food Chem.* **2019**, *292*, 325–335. [[CrossRef](#)] [[PubMed](#)]
53. LeCun, Y.; Bengio, Y.; Hinton, G. Deep learning. *Nature* **2015**, *521*, 436–444. [[CrossRef](#)] [[PubMed](#)]
54. Marco, S.; Gutierrez-Galvez, A. Signal and data processing for machine olfaction and chemical sensing: A review. *IEEE Sens. J.* **2012**, *12*, 3189–3214. [[CrossRef](#)]
55. Jolliffe, I.T.; Cadima, J. Principal component analysis: A review and recent developments. *Philos. Trans. R. Soc. A Math. Phys. Eng. Sci.* **2016**, *374*, 20150202. [[CrossRef](#)]
56. Sen, A.; Albarella, J.D.; Carey, J.R.; Kim, P.; McNamara, W.B. Low-cost colorimetric sensor for the quantitative detection of gaseous hydrogen sulfide. *Sens. Actuators B Chem.* **2008**, *134*, 234–237. [[CrossRef](#)]
57. Khorramifar, A.; Karami, H.; Wilson, A.D.; Sayyah, A.H.A.; Shuba, A.; Lozano, J. Grape cultivar identification and classification by machine olfaction analysis of leaf volatiles. *Chemosensors* **2022**, *10*, 125. [[CrossRef](#)]
58. Hayes, T.L.; Kanan, C. Lifelong machine learning with deep streaming linear discriminant analysis. In Proceedings of the IEEE/CVF Conference on Computer Vision and Pattern Recognition (CVPR), Seattle, WA, USA, 14–19 June 2020.
59. Gómez, A.H.; Hu, G.; Wang, J.; Pereira, A.G. Evaluation of tomato maturity by electronic nose. *Comput. Electron. Agric.* **2006**, *54*, 44–52. [[CrossRef](#)]
60. Choi, S.I.; Jeon, H.M.; Jeong, G.M. Data reconstruction using subspace analysis for gas classification. *IEEE Sens. J.* **2017**, *17*, 5954–5962. [[CrossRef](#)]
61. Palacín, J.; Rubies, E.; Clotet, E. Application of a Single-Type eNose to Discriminate the Brewed Aroma of One Caffeinated and Decaffeinated Encapsulated Espresso Coffee Type. *Chemosensors* **2022**, *10*, 421. [[CrossRef](#)]
62. Palacín, J.; Clotet, E.; Rubies, E. Assessing over Time Performance of an eNose Composed of 16 Single-Type MOX Gas Sensors Applied to Classify Two Volatiles. *Chemosensors* **2022**, *10*, 118. [[CrossRef](#)]
63. Chang, C.; Lin, C. A library for support vector machines. *TIST* **2011**, *2*, 1–27. [[CrossRef](#)]
64. Pardo, M.; Sberveglieri, G. Classification of electronic nose data with support vector machines. *Sens. Actuators B Chem.* **2005**, *107*, 730–737. [[CrossRef](#)]
65. Qiu, S.; Wang, J. The prediction of food additives in the fruit juice based on electronic nose with chemometrics. *Food Chem.* **2017**, *230*, 208–214. [[CrossRef](#)] [[PubMed](#)]
66. Va, B.; Subramoniam, M.; Mathew, L. Noninvasive detection of COPD and Lung Cancer through breath analysis using MOS Sensor array based e-nose. *Expert Rev. Mol. Diag.* **2021**, *21*, 1223–1233. [[CrossRef](#)]
67. Smulko, J.M.; Ionescu, R.; Granqvist, C.G.; Kish, L.B. Determination of gas mixture components using fluctuation enhanced sensing and the LS-SVM regression algorithm. *Metrol. Meas. Syst.* **2015**, *22*, 341–350.
68. Uçar, A.; Özalp, R. Efficient android electronic nose design for recognition and perception of fruit odors using Kernel Extreme Learning Machines. *Chemom. Intell. Lab. Syst.* **2017**, *166*, 69–80. [[CrossRef](#)]
69. Chen, L.; Wu, C.; Chou, T.-I.; Chiu, S.-W.; Tang, K.-T. Development of a dual MOS electronic nose/camera system for improving fruit ripeness classification. *Sensors* **2018**, *18*, 3256. [[CrossRef](#)] [[PubMed](#)]
70. Shi, Y.; Gong, F.; Wang, M.; Liu, J.; Wu, Y.; Men, H. A deep feature mining method of electronic nose sensor data for identifying beer olfactory information. *J. Food Eng.* **2019**, *263*, 437–445. [[CrossRef](#)]
71. Zhang, S.; Li, X.; Zong, M.; Zhu, X.; Wang, R. Efficient kNN classification with different numbers of nearest neighbors. *IEEE Trans. Neural Netw. Learn. Syst.* **2017**, *29*, 1774–1785. [[CrossRef](#)]
72. Schroeder, V.; Evans, E.D.; Wu, Y.C.M.; Voll, A.C.C.; McDonald, B.R.; Savagatrup, S.; Swager, T.M. Chemiresistive sensor array and machine learning classification of food. *ACS Sens.* **2019**, *4*, 2101–2108. [[CrossRef](#)] [[PubMed](#)]

73. Mirzaee-Ghaleh, E.; Taheri-Garavand, A.; Ayari, F.; Lozano, J. Identification of fresh-chilled and frozen-thawed chicken meat and estimation of their shelf life using an E-nose machine coupled fuzzy KNN. *Food Anal. Methods* **2020**, *13*, 678–689. [\[CrossRef\]](#)
74. Xu, Y.; Zhao, X.; Chen, Y.; Zhao, W. Research on a mixed gas recognition and concentration detection algorithm based on a metal oxide semiconductor olfactory system sensor array. *Sensors* **2018**, *18*, 3264. [\[CrossRef\]](#)
75. Quinlan, J.R. Induction of decision trees. *Mach. Learn.* **1986**, *1*, 81–106. [\[CrossRef\]](#)
76. Safavian, S.R.; Landgrebe, D. A survey of decision tree classifier methodology. *IEEE Trans. Syst.* **1991**, *21*, 660–674. [\[CrossRef\]](#)
77. Cho, J.; Li, X.; Gu, Z.; Kurup, P.U. Recognition of explosive precursors using nanowire sensor array and decision tree learning. *IEEE Sens. J.* **2011**, *12*, 2384–2391. [\[CrossRef\]](#)
78. Hassan, M.; Bermak, A. Gas classification using binary decision tree classifier. In Proceedings of the IEEE International Symposium on Circuits and Systems (ISCAS), Melbourne, VIC, Australia, 1–5 June 2014.
79. He, A.; Yu, J.; Wei, G.; Chen, Y.; Wu, H. Short-time Fourier transform and decision tree-based pattern recognition for gas identification using temperature modulated microhotplate gas sensors. *J. Sens.* **2016**, *2016*, 7603931. [\[CrossRef\]](#)
80. Breiman, L. Random forests. *Mach. Learn.* **2001**, *45*, 5–32. [\[CrossRef\]](#)
81. Wei, G.; Zhao, J.; Yu, Z.; Feng, Y.; Li, G.; Sun, X. An effective gas sensor array optimization method based on random forest. In Proceedings of the 2018 IEEE SENSORS, New Delhi, India, 28–31 October 2018.
82. Muhamad, N.A.; Musa, I.V.; Malek, Z.A.; Mahdi, A.S. Classification of partial discharge fault sources on SF₆ insulated switchgear based on twelve by-product gases random forest pattern recognition. *IEEE Access* **2020**, *8*, 212659–212674. [\[CrossRef\]](#)
83. Bogdal, C.; Schellenberg, R.; Lory, M.; Bovens, M.; Höpli, O. Recognition of gasoline in fire debris using machine learning: Part I, application of random forest, gradient boosting, support vector machine, and naïve bayes. *Forensic Sci. Int.* **2022**, *331*, 111146. [\[CrossRef\]](#)
84. Wu, X.; Kumar, V.; Ross Quinlan, J.; Ghosh, J.; Yang, Q.; Motoda, H.; McLachlan, G.J.; Ng, A.; Liu, B.; Yu, P.S.; et al. Top 10 algorithms in data mining. *Knowl. Inf. Syst.* **2008**, *14*, 1–37. [\[CrossRef\]](#)
85. Wijaya, D.R.; Sarno, R.; Daiva, A.F. Electronic nose for classifying beef and pork using Naïve Bayes. In Proceedings of the 2017 International Seminar on Sensors, Instrumentation, Measurement and Metrology (ISSIMM), Surabaya, Indonesia, 25–26 August 2017.
86. Grodnyomchai, B.; Chalapat, K.; Jitkajornwanich, K.; Jaiyen, S. A deep learning model for odor classification using deep neural network. In Proceedings of the 2019 5th International Conference on Engineering, Applied Sciences and Technology (ICEAST), Luang Prabang, Laos, 2–5 July 2019.
87. Pan, H.; He, S.; Zhang, T.; Song, S.; Wang, K. Application of an improved naive Bayesian analysis for the identification of air leaks in boreholes in coal mines. *Sci. Rep.* **2022**, *12*, 16081. [\[CrossRef\]](#)
88. Jian, Y.; Huang, D.; Yan, J.; Lu, K.; Huang, Y.; Wen, T.; Zeng, T.; Zhong, S.; Xie, Q. A novel extreme learning machine classification model for e-Nose application based on the multiple kernel approach. *Sensors* **2017**, *17*, 1434. [\[CrossRef\]](#)
89. Zhang, L.; Deng, P. Abnormal odor detection in electronic nose via self-expression inspired extreme learning machine. *IEEE Trans. Syst. Man Cybern. Syst.* **2017**, *49*, 1922–1932. [\[CrossRef\]](#)
90. Wang, T.; Zhang, H.; Wu, Y.; Chen, X.; Chen, X.; Zeng, M.; Yang, J.; Su, Y.; Hu, N.; Yang, Z. Classification and concentration prediction of VOCs with high accuracy based on an electronic nose using an ELM-ELM integrated algorithm. *IEEE Sens. J.* **2022**, *22*, 14458–14469. [\[CrossRef\]](#)
91. Xu, X.; Qin, H.; Zhou, J. Cyber Intrusion Detection Based on a Mutative Scale Chaotic Bat Algorithm with Backpropagation Neural Network. *Secur. Commun. Netw.* **2022**, *2022*, 5605404. [\[CrossRef\]](#)
92. Rumelhart, D.E.; Hinton, G.E.; Williams, R.J. Learning representations by back-propagating errors. *Nature* **1986**, *323*, 533–536. [\[CrossRef\]](#)
93. Mishra, V.N.; Dwivedi, R.; Das, R.R. Classification of gases/odors using dynamic responses of thick film gas sensor array. *IEEE Sens. J.* **2013**, *13*, 4924–4930.
94. Chu, J.; Li, W.; Yang, X.; Wu, Y.; Wang, D.; Yang, A.; Yuan, H.; Wang, X.; Li, Y.; Rong, M. Identification of gas mixtures via sensor array combining with neural networks. *Sens. Actuators B Chem.* **2021**, *329*, 129090. [\[CrossRef\]](#)
95. Benrekia, F.; Attari, M.; Bouhedda, M. Gas sensors characterization and multilayer perceptron (MLP) hardware implementation for gas identification using a field programmable gate array (FPGA). *Sensors* **2013**, *13*, 2967–2985. [\[CrossRef\]](#)
96. Yu, H.; Xie, T.; Paszczyński, S.; Wilamowski, B.M. Advantages of radial basis function networks for dynamic system design. *IEEE Trans. Ind. Electron.* **2011**, *58*, 5438–5450. [\[CrossRef\]](#)
97. Jiang, X.; Jia, P.; Luo, R.; Deng, B.; Duan, S.; Yan, J. A novel electronic nose learning technique based on active learning: EQBC-RBFNN. *Sens. Actuators B Chem.* **2017**, *249*, 533–541. [\[CrossRef\]](#)
98. Zhang, H.; Yu, X. Research on oil and gas pipeline defect recognition based on IPSO for RBF neural network. *Sustain. Comput. Inform. Syst.* **2018**, *20*, 203–209. [\[CrossRef\]](#)
99. Peng, P.; Zhao, X.; Pan, X.; Ye, W. Gas classification using deep convolutional neural networks. *Sensors* **2018**, *18*, 157. [\[CrossRef\]](#)
100. Pan, X.; Zhang, H.; Ye, W.; Bermak, A.; Zhao, X. A fast and robust gas recognition algorithm based on hybrid convolutional and recurrent neural network. *IEEE Access* **2019**, *7*, 100954–100963. [\[CrossRef\]](#)
101. Feng, L.; Dai, H.; Song, X.; Liu, J.; Mei, X. Gas identification with drift counteraction for electronic noses using augmented convolutional neural network. *Sens. Actuators B Chem.* **2022**, *351*, 130986. [\[CrossRef\]](#)
102. Wang, Y.; Diao, J.; Wang, Z.; Zhan, X.; Zhang, B.; Li, N.; Li, G. An optimized deep convolutional neural network for dendrobium classification based on electronic nose. *Sens. Actuators B Phys.* **2020**, *307*, 111874. [\[CrossRef\]](#)

103. Ma, D.; Gao, J.; Zhang, Z.; Zhao, H. Gas recognition method based on the deep learning model of sensor array response map. *Sens. Actuators B Chem.* **2021**, *330*, 129349. [[CrossRef](#)]
104. Xiong, Y.; Chen, Y.; Chen, C.; Wei, X.; Xue, Y.; Wan, H.; Wang, P. An odor recognition algorithm of electronic noses based on convolutional spiking neural network for spoiled food identification. *J. Electrochem. Soc.* **2021**, *168*, 077519. [[CrossRef](#)]
105. Zhao, X.; Wen, Z.; Pan, X.; Ye, W.; Bermak, A. Mixture gases classification based on multi-label one-dimensional deep convolutional neural network. *IEEE Access* **2019**, *7*, 12630–12637. [[CrossRef](#)]
106. Sharma, M.; Maity, T. Multisensor Data-Fusion-Based Gas Hazard Prediction Using DSET and 1DCNN for Underground Longwall Coal Mine. *IEEE Internet Things J.* **2022**, *9*, 21064–21072. [[CrossRef](#)]
107. Sun, Y.; Zhang, X. Tilapia freshness prediction utilizing gas sensor array system combined with convolutional neural network pattern recognition model. *Int. J. Food Prop.* **2022**, *25*, 2066–2072. [[CrossRef](#)]
108. Hochreiter, S.; Schmidhuber, J. Long short-term memory. *Neural Comput.* **1997**, *9*, 1735–1780. [[CrossRef](#)]
109. Zhang, W.; Wang, L.; Chen, J.; Xiao, W.; Bi, X. A novel gas recognition and concentration detection algorithm for artificial olfaction. *IEEE Trans. Instrum. Meas.* **2021**, *70*, 1–14. [[CrossRef](#)]
110. Wang, Q.; Qi, H.; Liu, F. Time Series Prediction of E-nose Sensor Drift Based on Deep Recurrent Neural Network. In Proceedings of the 38th Chinese Control Conference, Guangzhou, China, 27–30 July 2019.
111. Zou, Y.; Lv, J. Using recurrent neural network to optimize electronic nose system with dimensionality reduction. *Electronics* **2020**, *9*, 2205. [[CrossRef](#)]
112. Kwon, D.; Jung, G.; Shin, W.; Jeong, Y.; Hong, S. Low-power and reliable gas sensing system based on recurrent neural networks. *Sens. Actuators B Chem.* **2021**, *340*, 129258. [[CrossRef](#)]
113. Bakiler, H.; Güney, S. Estimation of Concentration Values of Different Gases Based on Long Short-Term Memory by Using Electronic Nose. *Biomed. Signal Process. Control* **2021**, *69*, 102908. [[CrossRef](#)]
114. Lobo, J.L.; Del, S.J.; Bifet, A.; Kasabov, N. Spiking neural networks and online learning: An overview and perspectives. *Neural Netw.* **2020**, *121*, 88–100. [[CrossRef](#)]
115. Jing, Y.; Meng, Q.; Qi, F.; Cao, M.; Zeng, M.; Ma, S. A bioinspired neural network for data processing in an electronic nose. *IEEE Trans. Instrum. Meas.* **2016**, *65*, 2369–2380. [[CrossRef](#)]
116. Sarkar, S.T.; Bhondekar, A.P.; Macaš, M.; Kumar, R.; Kaur, R.; Sharma, A.; Gulati, A.; Kumar, A. Towards biological plausibility of electronic noses: A spiking neural network based approach for tea odour classification. *Neural Netw.* **2015**, *71*, 142–149. [[CrossRef](#)]
117. Han, J.K.; Kang, M.; Jeong, J.; Cho, I.; Yu, J.; Yoon, K.; Park, I.; Choi, Y. Artificial Olfactory Neuron for an In-Sensor Neuromorphic Nose. *Adv. Sci.* **2020**, *9*, 2106017. [[CrossRef](#)]
118. Kwon, D.; Jung, G.; Shin, W.; Jeong, Y.; Hong, S.; Oh, S.; Kim, J.; Bae, J.; Park, B.; Lee, J. Efficient fusion of spiking neural networks and FET-type gas sensors for a fast and reliable artificial olfactory system. *Sens. Actuators B Chem.* **2021**, *345*, 130419. [[CrossRef](#)]

Disclaimer/Publisher's Note: The statements, opinions and data contained in all publications are solely those of the individual author(s) and contributor(s) and not of MDPI and/or the editor(s). MDPI and/or the editor(s) disclaim responsibility for any injury to people or property resulting from any ideas, methods, instructions or products referred to in the content.